

FIG. 7. Postoperative findings at 7 months after surgery. (Left) In the radiographic findings, satisfactory bone union and alignment was observed. (Right) The patient can walk without a cane, and full weight bearing is possible.

bone graft can be double-barreled without disturbing its blood supply.^{6,7} The double-barreled fibular graft can provide enough strength to support the spinal column.

Various methods of fixation can be considered. The standard method involves internal fixation with screws and a plate combined with external plaster casting. However, the start of walking rehabilitation is often delayed with this method, and long-term fixation can decrease postoperative quality of life. Prolonged rehabilitation is a significant problem for patients, especially for those with a poor prognosis. External skeletal fixation can also be used; although this method does not require internal devices, the instrumentation is too bulky for pelvic fixation. As we have reported earlier, we previously used screws and a plate for fixation of the transferred bone graft.⁶ However, more recently, our first choice of fixation device has been the Cotrel-Dubousset rod system.

The Cotrel-Dubousset rod system was originally developed to treat spinal scoliosis.⁸ The most recent version of the system consists of a rod and pedicular screws and can be used for internal fixation of traumatic lesions of the spine and for pelvic ring reconstruction.⁹⁻¹¹ The transferred bone can be rigidly fixed by compression pressure along the rod. The rigid fixation allows early rehabilitation of walking. A possible disadvantage is the dead space caused by the relatively large device, which sometimes requires soft-tissue coverage, such

as with a rectus abdominis musculocutaneous flap or latissimus dorsi musculocutaneous flap.

CONCLUSIONS

The double-barreled fibular graft is well vascularized and can achieve satisfactory bone union. It is a safe and effective method for reconstructing the pelvic ring. Furthermore, the Cotrel-Dubousset rod system can provide rigid fixation soon after surgery and is useful for early rehabilitation of walking.

Minoru Sakuraba, M.D., Ph.D.

Division of Plastic and Reconstructive Surgery
National Cancer Center Hospital East

6-5-1 Kashiwanoha Kashiwa-City, Chiba 277-8577, Japan

msakurab@east.ncc.go.jp

REFERENCES

1. Enneking, W. F., and Dunham, W. K. Resection and reconstruction for primary neoplasms involving the innominate bone. *J. Bone Joint Surg. (Am.)* 60: 731, 1978.
2. Enneking, W. F., Dunham, W., Gebhardt, M. C., et al. A system for the functional evaluation of reconstructive procedures after surgical treatment of tumors of the musculoskeletal system. *Clin. Orthop.* 286: 241, 1993.
3. O'Connor, M. I., and Sim, F. H. Salvage of the limb in the treatment of malignant pelvic tumors. *J. Bone Joint Surg. (Am.)* 71: 481, 1989.
4. Huth, J. F., Eckardt, J. E., Pignatti, G., and Eilber, F. Resection of malignant bone tumors of the pelvic girdle without extremity amputation. *Arch. Surg.* 123: 1121, 1988.
5. Leung, P. C. Reconstruction of the pelvic ring after tumor resection. *Int. Orthop.* 16: 168, 1992.

6. Iida, H., Hata, Y., Kimata, Y., et al. Pelvic ring reconstruction with twin-barrel vascularized fibular bone graft. *J. Jpn. Soc. Reconstr. Microsurg.* 13: 43, 2000.
7. Jones, N. F., Swartz, W. M., Mears, D. C., Jupiter, J. B., and Grossman, A. The "double barrel" free vascularized fibular bone graft. *Plast. Reconstr. Surg.* 81: 378, 1988.
8. Hopf, C. G., Eysel, P., and Dubousset, J. Operative treatment of scoliosis with Cotrel-Dubousset instrumentation: New anterior spinal device. *Spine* 22: 618, 1997.
9. Oka, S., Ohara, T., Niyatake, S., et al. Reconstruction of pelvic ring after resection of malignant pelvic bone tumor. *J. West. Jpn. Res. Soc. Spine* 24: 203, 1998.
10. Abumi, K., Takeda, N., Minami, A., et al. Reconstruction of the pelvic ring using Isola spinal system. *J. Joint Surg.* 17: 68, 1998.
11. Nagoya, S., Usui, M., and Ishii, S. Reconstruction of the pelvis by free vascularized fibular graft following resection of malignant tumor. *J. Joint Surg.* 18: 68, 1999.

Short Pedicle Superficial Inferior Epigastric Artery Adiposal Flap: New Anatomical Findings and the Use of This Flap for Reconstruction of Facial Contour

Isao Koshima, M.D.

Tokyo, Japan

Free vascularized dermal-fat flaps have been used for facial contouring in the treatment of congenital and traumatized facial atrophy. The major disadvantages of these flaps are wide postoperative donor scars and bulkiness of the transferred flaps. To overcome these disadvantages, we previously reported on the intraoral transfer of a deep inferior epigastric artery perforator (DIEP) adiposal flap based on only a perforator. Although many shortcomings with this flap have been overcome, detection and dissection for paraumbilical perforators are still difficult. To overcome these shortcomings for facial contour correction, we have used a superficial inferior epigastric artery adiposal flap with one-stage removal of bulky fatty tissue. This article describes new anatomical findings regarding the superficial inferior epigastric artery system and successful use of an intraorally or extraorally transferred superficial inferior epigastric artery adiposal flap with a short pedicle for three patients with facial contour deformities.

ANATOMY

On the basis of an anatomical study of 10 cadavers and more clinical cases, it was observed that the superficial inferior epigastric artery divides from the femoral artery below the inguinal ligament and runs superiorly to approach the umbilicus. This branch locates

proximally over the deep fascia of the rectus abdominis muscle and distally in the superficial fatty layer. It gives off a few cutaneous perforators (0.3 to 0.5 mm in diameter) during the whole course. The superficial or deep branch of the superficial circumflex iliac artery also derives from the femoral artery and runs in a superolateral direction over or under the deep fascia of the sartorius muscle through the inguinal ligament. The superficial circumflex iliac artery system gives off several ascending branches to connect the superficial inferior epigastric artery system in the lower abdominal region.

Sometimes, on the basis of our cadaveric and clinical experiences, in cases where the superficial inferior epigastric artery is absent or hypoplastic, long, large ascending branches of the superficial circumflex iliac artery system develop complementarily. When a superficial inferior epigastric artery is long and large, the ascending branches of the superficial circumflex iliac artery system are usually short and small. Both systems complement each other in the lower abdominal region. The distal terminals of the superficial inferior epigastric artery sometimes connect to the perforators from the deep inferior epigastric system. Regarding the venous drainage of the superficial inferior epigastric artery system, the superficial epigastric vein is part of the large cutaneous venous sys-

From the Department of Plastic and Reconstructive Surgery, Graduate School of Medicine, University of Tokyo. Received for publication August 9, 2004.

Presented in part at the Second World Symposium of Reconstructive Microsurgery, in Heidelberg, Germany, June 12, 2003, and at the 12th International Conference of Plastic, Reconstructive, and Aesthetic Surgery, in Sydney, Australia, August 14, 2003.

DOI: 10.1097/01.prs.0000178794.11828.49

tem in this area, which always exists and often runs independently medial (and sometimes parallel) to the superficial inferior epigastric artery system in the superficial layer of fatty tissue. The major superficial inferior epigastric artery trunk usually does not have the concomitant veins, but sometimes it is accompanied by tiny concomitant veins (<0.5 mm). The three-dimensional distributions of the superficial inferior epigastric artery, its concomitant vein, and the superficial epigastric vein are complicated. The superficial vein distributes through the subdermal layer, and the superficial inferior epigastric artery and its concomitant vein are in the deep layer of the superficial fatty layer above the superficial fascia in the lower abdominal wall (Fig. 1).

FLAP ELEVATION

Although preoperative Doppler examination is useful for confirming the course of the superficial inferior epigastric artery, the sounds do not correlate with the size of the artery because even very small arteries of less than 0.3 mm can produce strong sounds. The flap is outlined to include the superficial inferior epigastric artery. The first incision is made transversely through the inguinal ligament to detect the existence and size of the superficial inferior epigastric artery and superficial epigastric vein. In some cases where the superficial inferior epigastric artery is small (<0.3 mm) or

absent, the ascending branch of the superficial circumflex iliac artery system is usually detected. When a superficial inferior epigastric artery is very large, the superficial circumflex iliac artery ascending branch is usually small or absent. Therefore, either dominant artery can be selected as a pedicle of the superficial inferior epigastric artery flap. The superficial epigastric vein is always present and runs 3 cm medially through the superficial inferior epigastric artery.

After confirming locations of the superficial inferior epigastric artery (or the ascending branch) and superficial epigastric vein, a flap is outlined on the lower abdominal wall. The selected pedicle artery is placed at the proximal end of the adiposal flap. Then, a transverse skin incision is extended through the inguinal ligament to include the distal pedicle artery above the deep fascia. After a whole adiposal flap is incised and elevated subcutaneously, the proximal portion of the pedicle vessel is transected just above the inguinal ligament and a superficial inferior epigastric artery adiposal flap is obtained. Proximal dissection of the pedicle vessel to the femoral artery is not necessary. Pedicle vessels (superficial inferior epigastric artery or ascending branch, and superficial epigastric vein) are usually transected just above the inguinal ligament.

To achieve adequate thickness of the flap, it can be thinned primarily by resection of the

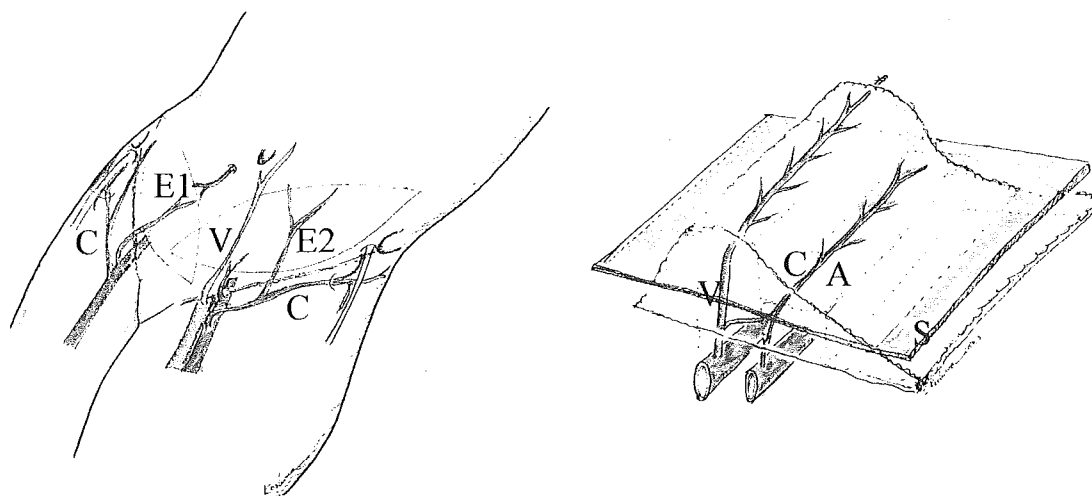


FIG. 1. (Left) Schematic drawing of the superficial inferior epigastric arterial system. The superficial inferior epigastric artery usually arises from the femoral artery just below the inguinal ligament (E1) and joins with the perforators of the deep inferior epigastric artery system. The superficial inferior epigastric artery (E2) is sometimes missing and arises from the superficial circumflex iliac artery (C), as in the left groin region. V, superficial epigastric vein. (Right) Schema of the three-dimensional distribution of the superficial inferior epigastric artery (A), its concomitant vein (C), and the superficial epigastric vein (V). S, superficial fascia in the lower abdominal wall.

superficial portion of the fatty tissue from the flap to not damage the superficial epigastric vein, because the superficial inferior epigastric artery is located in the deep adiposal layer and the superficial epigastric vein in the superficial layer. If necessary, thinning, except around the perforator in the flap, is possible with removal of fatty tissue with scissors. The key point for this operation is bloodless flap elevation to detect and preserve the distal branches of the superficial inferior epigastric artery or superficial circumflex iliac artery branches. Finally, the donor abdominal defect is closed primarily by direct closure with suction drainage. A postoperative pressure bandage is required for 2 weeks (Fig. 1).

CASE REPORTS

Between May of 2002 and March of 2004, the facial deformities of six patients were repaired with a free superficial inferior epigastric artery adiposal flap with a short pedicle. The patients ranged in age from 11 to 53 years (all were female patients). Two cases involved facial lipodystrophy, two had hemifacial hyperplasia, one had a postmaxillectomy deformity, and one experienced forehead depression after a fracture involving the skull base. The flap was implanted by an intraoral approach in three cases for buccal augmentation. Regarding selection of the recipient vessels, the facial artery and its branch, the superficial temporal artery and its preauricular branch, the facial vein or a concomitant vein of the facial artery, and the superficial temporal vein were used. Postoperatively, blood circulation of the adiposal flap was confirmed by continuous bleeding at the distal side of the flap. Postoperative patency of the anastomosed flap artery was detected by a Doppler audiometer, and there was no postoperative reexploration of the anastomosed vessels because of thrombosis. None of the cases experienced postoperative infection or donor site problems (Table I).

Case 1: Free Superficial Inferior Epigastric Artery Adiposal Flap for Facial Lipodystrophy (Intraoral Approach)

A 46-year-old woman with localized lipodystrophy of the right side of her face complained of a right cheek depression. A subcutaneous pocket was created supraperiosteally in the right cheek through an intraoral mucosal incision. With a small submandibular incision 2 cm in length, the right facial vessels were exposed as recipient vessels. Through a medial

longitudinal scar on the lower abdominal wall following hysterectomy, the superficial inferior epigastric artery and superficial epigastric vein were dissected. A free superficial inferior epigastric artery adiposal flap, 8 × 8 cm, was elevated and primary thinning of the flap was performed. The pedicle vessels, superficial inferior epigastric artery, and superficial epigastric vein were anastomosed to the right facial vessel. The abdominal donor defect was closed directly.

Temporary facial palsy and trigeminal sensory loss occurred around the right upper lip for 1 week. Two years after surgery, there was no atrophy of the augmented face (Fig. 2).

Case 2: Free Superficial Inferior Epigastric Artery–Superficial Circumflex Iliac Artery Adiposal Flap for Postoperative Facial Deformity

A 53-year-old woman presented with a depressed right malar region. Thirty-three years earlier, she had received surgical treatment for right maxillary sinusitis. Thereafter, her facial deformity had occurred. A three-dimensional computed tomographic scan revealed depression of the anterior wall of the maxillary bone.

After creating a subperiosteal pocket through subciliary and alar incisions on the right side of the face, the superficial temporal vessel was exposed through a preauricular incision as a recipient vessel. Through a previous operative scar on the right abdominal wall, the pedicle vessels were dissected to elevate an adiposal flap. As the superficial inferior epigastric artery was very small (0.7 mm), the ascending branch of the superficial circumflex iliac artery (1.0 mm) was included in the flap.

A free adiposal flap, 13 × 7 cm, was transferred to the prepared face, and fatty tissue was removed to reduce the thick flap. The pedicle arteries of the flap, the superficial inferior epigastric artery (0.7 mm) and the superficial circumflex iliac artery (1.0 mm), were respectively joined to the preauricular branch (0.7 mm) and parietal branch (1.0 mm) of the superficial temporal artery. The superficial epigastric vein (1.5 mm) of the flap was anastomosed to the superficial temporal vein.

Her postoperative course was without problems. There was no flap necrosis and, 7 years 7 months after surgery, the patient had a nearly normal malar contour with additional surgery. She had no problems in the donor abdominal wall (Fig. 3).

Case 3: Free Superficial Inferior Epigastric Artery Adiposal Flap for Hemifacial Microsomia

A 14-year-old girl with hemifacial microsomia of the right face complained of facial asymmetry caused by hypoplasia of the facial and mandibular bones and soft tissues. Using an intraoral approach with a sulcus incision, subperiosteal and subcutaneous

TABLE I
Patient Summary: Superficial Inferior Epigastric Artery Adiposal Flap

Case	Age (yr)/Sex	Diseases	Recipient-Anastomosed Vessels	Complications
1	46/F	Lipodystrophy	FA-SIEA, FA branch–SIEA branch, SIEV-FV	–
2	53/F	Maxillary carcinoma postoperative deformity	STA-SCIA, STA preauricular branch–SIEA, SIEV-FV	–
3	14/F	Hemifacial hypoplasia	FA-SIEA, SIEV-FA concomitant vein	–
4	19/F	Established forehead fracture	SIEA T portion-STA (flow-through), SIEV-STV	–
5	11/F	Hemifacial microsomia	FA-SCIA ascending branch, SCIV-FV	–

FA, facial artery; FV, facial vein; SIEA, superficial inferior epigastric artery; SIEV, superficial inferior epigastric vein; STA, superficial temporal artery; STV, superficial temporal vein; SCIA, superficial circumflex iliac artery; SCIV, superficial circumflex iliac vein.

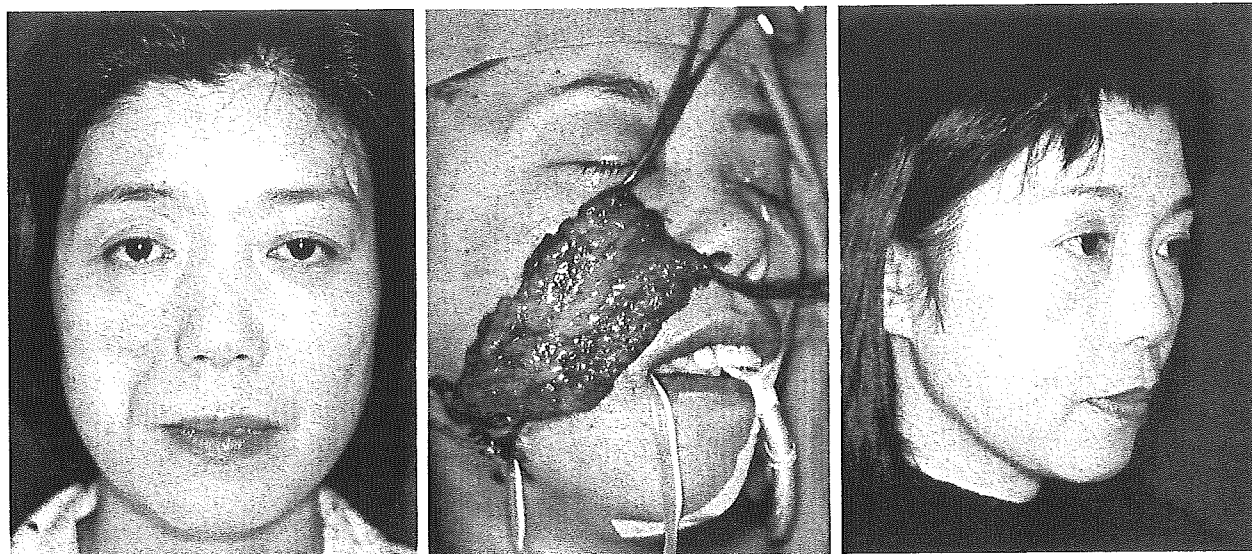


FIG. 2. (Left) Preoperative frontal view of a 46-year-old woman with right facial lipodystrophy (the patient in case 1). (Center) A free superficial inferior epigastric artery adiposal flap obtained from her left abdominal wall was transferred intraorally. (Right) Postoperative lateral view 1 year 9 months after surgery. No additional surgery was required.

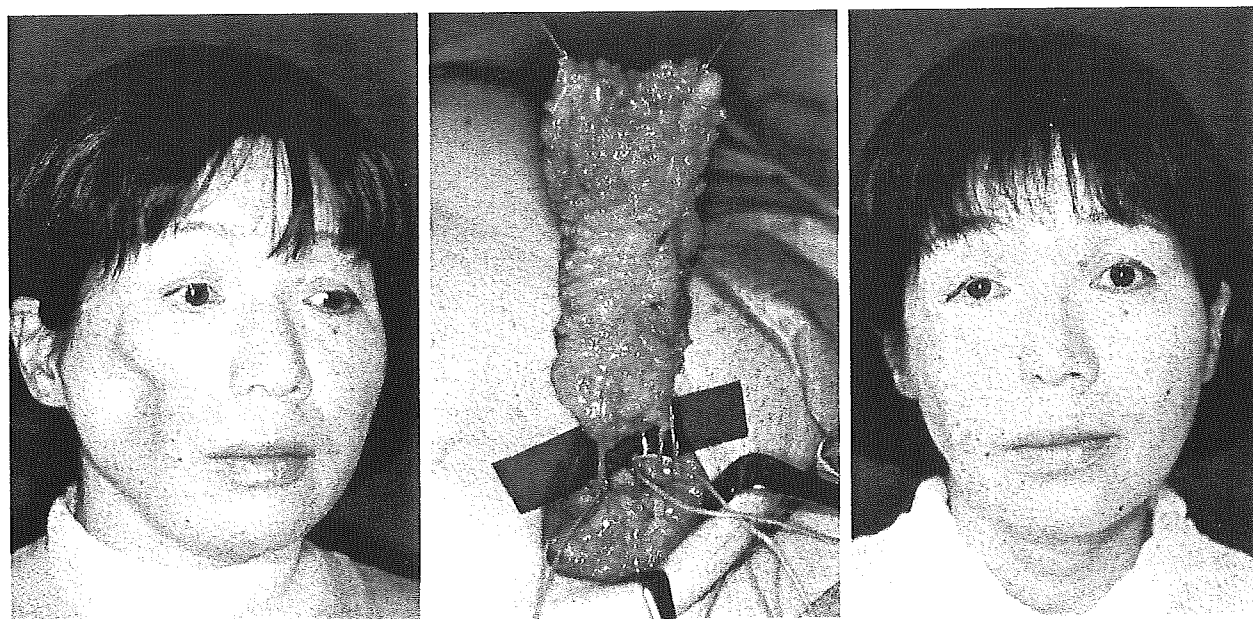


FIG. 3. (Left) Preoperative lateral view of a 53-year-old woman (the patient in case 2) with right malar depression after maxillary resection. (Center) An intraoperative customized (debunked) superficial inferior epigastric artery adiposal flap with a short pedicle transected above the inguinal ligament. (Right) Postoperative view 1 year 4 months later.

dissection was performed to create a subcutaneous pocket in the right cheek. The facial vessel in the affected face, which showed no anatomical irregularity, was prepared as a recipient vessel. A superficial inferior epigastric artery adiposal flap, 10×5 cm, was obtained through a small transverse incision in the right lower abdominal wall. The large superficial inferior epigastric artery and superficial epigastric vein were transected above the inguinal ligament. The proximal end of the pedicle vessel of this flap was anastomosed to the facial vessel through a very small (3 cm in length) submandibular incision. The donor defect was closed directly.

The patient's postoperative course was smooth. One year 4 months after surgery, there was no infection of the flap, and

no additional defatting or augmentation of the repaired face was required. The donor site showed no complications such as abdominal hernia, weakness, bulging, or related lumbago (Figs. 4 and 5).

DISCUSSION

Historically, a free deltopectoral dermal-fat flap was first used for hemifacial atrophy patients.^{1,2} Since then, a vascularized groin dermal-fat flap^{2,3} has become popular as the first choice for this correction. These established



FIG. 4. (*Left*) Preoperative frontal view of a 14-year-old girl with a right hemifacial hypoplasia (the patient in case 3). (*Right*) Postoperative frontal view 13 months after flap transfer; with no additional surgery.

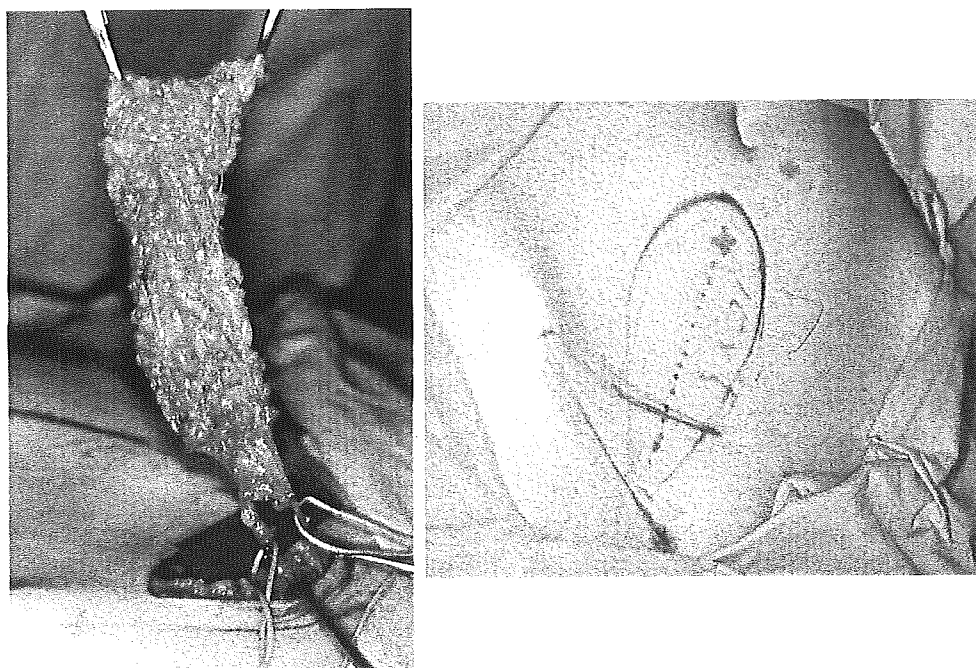


FIG. 5. (*Left*) A superficial inferior epigastric artery adiposal flap was designed on the right lower abdomen. (*Right*) An adiposal flap was elevated to be transferred intraorally, with a minimal submandibular incision.

dermal-fat flaps contain hard subcutaneous tissue, which results in scar formation of the transferred subcutaneous dermis. In addition, a large dermal-fat flap requires donor-site skin grafting, which causes poor aesthetic results in the donor region.

After the introduction of scapular and parascapular flaps,^{5,6} a customized parascapular flap⁷⁻¹⁰ with extension of the dorsal thoracic fascia and/or inframammary fascia was developed for facial contour correction. This flap has the advantage of customized thickness for

one-stage reconstruction. However, simultaneous flap elevation is difficult because the donor site is close to the face and also a change in position may be necessary to obtain the flap. In addition, the donor scar is unacceptable for young women.

To overcome these disadvantages of established flaps, we developed a DIEP adiposal flap¹¹⁻¹⁴ without the rectus abdominis muscle and paraumbilical perforator adiposal flap, with a short perforator and an intraoral approach,¹⁵ and these have been applied to facial contour correction.⁴ These flaps result in minimum donor-site morbidity compared with a rectus abdominis musculocutaneous flap, and a considerable amount of the fatty tissue in these adiposal flaps can be removed. However, the disadvantage of the DIEP flap and paraumbilical flap is difficult dissection of the perforators and the deep inferior epigastric vessel through or above the rectus abdominis muscle.

On the basis of our cases, the superficial inferior epigastric artery flap seems to be more suitable for augmentation of facial contour deformities and large or thick soft-tissue defects in the head and neck region than rectus abdominis musculocutaneous, DIEP, or paraumbilical adiposal flaps. Allen and Heitland also used this flap for breast reconstructions.¹⁶ It leaves a more acceptable secondary defect for greater tissue yield than the scapular, parascapular, or other flaps. The advantages of the superficial inferior epigastric artery adiposal flap are as follows: (1) deeper and longer dissection of the superficial inferior epigastric artery system to the femoral artery as in the groin flap is unnecessary; (2) only a short length of the superficial inferior epigastric artery is required to nourish the flap; (3) flap elevation time is short; (4) thinning of the flap may be performed with primary defatting; (5) the bulky fat of this flap can be reduced with primary defatting, and customized defatting in one-stage reconstruction is possible; (6) it can be obtained at the aesthetically best donor site and results in minimum donor-site morbidity and a concealed donor scar; (7) preservation of the rectus abdominis muscle allows for pregnancy in young women; and (8) a large cutaneous vein, the superficial epigastric vein, is available as a venous drainage system.

The major disadvantage of a superficial inferior epigastric artery adiposal flap is anatomical variation: loss of the superficial inferior epigastric artery (or hypoplasia). Taylor found the

artery to be present in 65 percent of subjects in his study of groin dissections in cadavers.¹⁷ Allen and Heitland also found a consistency of 72 percent in dissected groins, and the artery was present on both groins in 58 percent.¹⁶ On the basis of our experiences, patients without a superficial inferior epigastric artery always have dominant ascending branches of the superficial circumflex iliac artery that supply the lower abdominal wall. Regarding the anatomy of the superficial inferior epigastric artery system, we believe that the ascending branch of the superficial circumflex iliac artery compensates for the superficial inferior epigastric artery deficit, and a superficial inferior epigastric artery flap can be raised in all patients with the superficial inferior epigastric artery itself or with an ascending branch of the superficial circumflex iliac artery and large superficial epigastric vein system. Another disadvantage is the fact that fine technical skills are necessary to dissect and anastomose the small and short pedicle vessels for the superficial inferior epigastric artery flap with a short pedicle. For beginners, a larger and longer vascular pedicle can be obtained including the proximal division (1.0 to 2.0 mm in diameter) of the superficial inferior epigastric artery from the femoral artery. Also, careless creation of a subcutaneous pocket in the face may result in damage to the buccal branches of the facial nerve. Finally, this flap seems to be the best application for facial contouring surgery, and it is indicated especially for children and for young women who expect to become mothers.

CONCLUSIONS

The major disadvantages of vascularized dermal-fat flaps for facial contouring in the treatment of congenital or traumatized facial asymmetries are postoperative wide donor scars and bulkiness of the transferred flaps. To overcome these disadvantages, we developed a superficial inferior epigastric artery adiposal flap with a short pedicle. This article describes new anatomical findings on the superficial inferior epigastric artery system and the successful use of an intraorally or extraorally transferred superficial inferior epigastric artery adiposal flap with a short pedicle for three patients with facial contour deformities. The advantages of this method are as follows: one-stage augmentation with a short transverse incision on the lowest part of the abdomen, and transfer through an intraoral or extraoral approach re-

sulting in a minimal incision on the face. The disadvantages are the anatomical variation of the superficial inferior epigastric artery, which can be compensated for by the ascending branch of superficial circumflex iliac artery, and difficult dissection of small-pedicle vessels.

Isao Koshima, M.D.

Department of Plastic and Reconstructive Surgery
Graduate School of Medicine

University of Tokyo

7-3-1, Hongo, Bunkyo-ku

Tokyo 113-8655, Japan

koushimai-pla@h.u-tokyo.ac.jp

ACKNOWLEDGMENTS

This study was supported in part by research project grant 11-202 from the Japan Ollily Company, and a grant-in-aid for cancer research from the Japanese Ministry of Health and Welfare. The authors thank Dr. Joji Tada, Department of Dermatology of Okayama City Hospital, and Dr. Michiya Kosaka, Department of Otolaryngology of Okayama University, for their support of this work.

REFERENCES

1. Fujino, T., Tanino, R., and Sugimoto, C. Microvascular transfer of free deltopectoral dermal-fat flap. *Plast. Reconstr. Surg.* 55: 428, 1975.
2. Shintomi, Y., Ohura, T., Honda, K., and Iida, K. The reconstruction of progressive facial hemi-atrophy by free vascularized dermis-fat flaps. *Br. J. Plast. Surg.* 34: 398, 1981.
3. Harashina, T., Nakajima, T., and Yoshimura, Y. A free groin flap reconstruction in progressive facial hemi-atrophy. *Br. J. Plast. Surg.* 30: 14, 1977.
4. Koshima, I., Inagawa, K., Urushibara, K., and Moriguchi, T. One-stage facial contour augmentation with intraoral transfer of a paraumbilical perforator adiposal flap. *Plast. Reconstr. Surg.* 108: 988, 2001.
5. Stern, H. S., Elliott, L. F., and Beegle, P. H. Progressive hemifacial atrophy associated with Lyme disease. *Plast. Reconstr. Surg.* 90: 579, 1992.
6. Upton, J., Albin, R. E., Mulliken, J. B., and Murray, J. E. The use of scapular and parascapular flaps for cheek reconstruction. *Plast. Reconstr. Surg.* 90: 959, 1992.
7. Longaker, M. T., and Siebert, J. W. Microvascular free-flap correction of severe hemifacial atrophy. *Plast. Reconstr. Surg.* 96: 800, 1995.
8. Siebert, J. W., Anson, G., and Longaker, M. T. Microsurgical correction of facial asymmetry in 60 consecutive cases. *Plast. Reconstr. Surg.* 97: 354, 1996.
9. Longaker, M. T., and Siebert, J. W. Microsurgical correction of facial contour in congenital craniofacial malformations: The marriage of hard and soft tissue. *Plast. Reconstr. Surg.* 98: 942, 1996.
10. Longaker, M. T., Flynn, A., and Siebert, J. W. Microsurgical correction of bilateral facial contour deformities. *Plast. Reconstr. Surg.* 98: 951, 1996.
11. Koshima, I., and Soeda, S. Inferior epigastric artery skin flaps without rectus abdominis muscle. *Br. J. Plast. Surg.* 42: 645, 1989.
12. Allen, R. J., and Treece, P. Deep inferior epigastric perforator flap for breast reconstruction. *Ann. Plast. Surg.* 32: 32, 1994.
13. Blondeel, P. N., and Boeckx, W. D. Refinements in free flap breast reconstruction: the free bilateral deep inferior epigastric perforator flap anastomosed to the internal mammary artery. *Br. J. Plast. Surg.* 47: 495, 1994.
14. Koshima, I., Inagawa, K., Urushibara, K., Ohtsuki, M., and Moriguchi, T. Deep inferior epigastric perforator dermal-fat or adiposal flap for correction of craniofacial contour deformities. *Plast. Reconstr. Surg.* 106: 10, 2000.
15. Koshima, I., Inagawa, K., Urushibara, K., and Moriguchi, T. Paraumbilical perforator flap without deep inferior epigastric vessels. *Plast. Reconstr. Surg.* 102: 1052, 1998.
16. Allen, R. J., and Heitland, A. S. Superficial inferior epigastric artery flap for breast reconstruction. *Semin. Plast. Surg.* 16: 35, 2002.
17. Taylor, G. I. The anatomy of several free flap donor sites. *Plast. Reconstr. Surg.* 56: 243, 1975.

Sequential Histological Examination and Morphometric Analysis of Osteogenesis in the Pores of Porous Hydroxyapatite with Attachment of Vascularized Periosteum

Akiko HIRATA, M.D.^{*}, Akiteru HAYASHI, M.D.^{**} and Yu MARUYAMA, M.D.^{*}

^{*} *Department of Plastic and Reconstructive Surgery, Toho University, School of medicine*

^{**} *Department of Plastic and Reconstructive Surgery, Toho University, Sakura Hospital*

Abstract

To elucidate the sequential changes of osteogenesis in pores of periosteum-attached hydroxyapatite blocks with a relationship to attachment of periosteum in the rabbit model, detailed microscopic observations and morphometric analysis of pores were carried out. Neither bone nor adipose tissue was found in the pores of PHAB embedded in the muscle during the entire experimental period in the control group. By contrast, newly formed bone tissue was confirmed to have a laminated architecture and depolarization was initially found at the margin of the pores near the face attached to by periosteum of rectangular-shaped PHAB at week 8, and bone formation in pores extended to the distal portion from the attached face. At week 12, adipose tissue was observed inside the bone, recognized as bone sloughing lining the pore. Morphometric analysis revealed a negative correlation of -0.279 ($p < 0.001$, $n = 1038$) between the percentage of bone in each pore and the distance from the face of PHAB attached periosteum.

The result suggested that bone-sloughing formation lining pores, filled by adipose tissue with islets of erythroblasts is induced by the differentiation of mesenchymal stem cells provided via periosteum attaching onto the face of PHAB. We wish to emphasize that the complex of PHAB-attached vascularized periosteum presented might provide a favorable and secure material for bone reconstruction *in vivo*.

Introduction

Autologous bone graft, especially vascularized bone graft, has been regarded as one of the most reliable and well documented procedures to repair defects after major surgical interventions or trauma^{1,2)}. However, it is hard to apply this graft for a larger defect because

it is essentially limited to obtain a sufficient volume of autologous bone grafting and work into various shapes for filling the defect. Hence, various materials have recently been proposed for substitutions, replacing autologous bone graft. Especially, whereas hydroxyapatite (HA) has been regarded as a promising candidate of artificial bone because

of its suitable biological affinity, clinical application of porous HA (PHA) is limited because of the difficulty to establish sufficient strength to replace the defect and prevent infection.

To overcome these drawbacks of PHA, we have highlighted vascularized periosteum^{3~6)}, and been investigating the possibility of the clinical use of PHA with the attachment of vascularized periosteum as an artificial bone that is generally known as a promoter of osteogenesis. This procedure can not only reduce invasiveness but obtain adjustable shapes of the graft for individual defects. Concise results of bone formation in pores of PHA and its usage have previously been discussed, however, osteogenesis and extension within the PHA block (PHAB) is still unclear because there few have been reports on detailed histological observations and sequential changes of bone formation in pores. To provide details of osteogenesis in pores of PHAB with the attachment of periosteum, the present paper describes sequential changes and extension of newly developed bone in pores of PHAB, and discusses osteogenesis with reference to previous reports.

Materials and Methods

1. Animals

Japanese white rabbits (male, approximately 3 kg in body weight) were raised under identical conditions and used for the following experiment. Animals that had infections or injured themselves during the rearing period were excluded from the experiment. Animals were handled in a humane way throughout the experimental period, in accordance with the Guideline for Animal Experiments of Toho University.

2. Preparation of rib-latissimus dorsi periosto-

muscle flaps and periosteum-attached porous hydroxyapatite blocks (PHAB)

Anesthesia was introduced and maintained by 25 mg/kg of pentobarbital sodium injection (Nembutal injection[®], Dainippon Pharmaceutical Co., Ltd., Osaka) administered into the auricular vein of the animals. Japanese white rabbits in the right lateral decubitus position were extensively shaved from the left forelimb to the lumbar region. A rectangle of approximately 40 × 90 mm in area was drawn on the surface of the overlying skin between the 8th and 10th ribs, 20 mm ventral to the spine, and the crossover site of the scapula and the posterior margin of the forelimb was included in the base of the flap to capture the origin of thoracodorsal blood vessels. A transverse linear incision was made to the latissimus dorsi muscle. The latissimus dorsi was cut anteriorly and posteriorly along the line, and the caudal end of the latissimus dorsi was cut and raised to expose the inferior margin of the 11th rib. The anterior portion of the rib-periosteum was detached from the rib, preserving the connection between the posterior aspect of the latissimus dorsi and periosteum. Thus, two or three strips of periosteum, each 3-5mm in width and 25-30 mm in length, were obtained from the 8th to the 11th ribs. Sterilized porous HA blocks⁷⁾ of 8 × 4 × 2 mm size (50% porosity, pore diameter 500 μm) (Apacerum[®], PENTAX, Tokyo) were attached firmly to the 8th and 9th rib-periosteum (canbium layer side) with 5-0 nylon thread and also attached to the posterior surface of the latissimus dorsi between strips of periosteum. A silicon film (Opsite[®], Smith & Nephew, USA) was sewn on the surface of the site where the latissimus dorsi flap was collected in order to block the influence of underlying ribs and intercostal muscles, and then, the muscle layer and skin were closed

with a two-layered suture in the usual manner (Fig. 1). To prevent infection after the surgical intervention, 100 mg/kg of piperacillin sodium (Pemmalin for injection[®], Sawai Pharmaceutical Co., Ltd., Osaka) was subcutaneously administered and 50 mg/kg of kanamycin sulfate (Kanamycin sulfate for injection "Meiji"[®], Meiji Seika Kaisha, Ltd., Tokyo) was intramuscularly administered to the animals.

Four rabbits each were sacrificed under intravenous anesthesia at 4, 8, and 12 weeks after the operation, and HA blocks with the surrounding tissues were extracted.

3. Histological examination and morphometric evaluation

The extracted samples were subjected to Villanueva bone staining following formalin fixation and then non-decalcified ground sections of 15 μ m thickness were prepared. These sections were observed under a light microscope, polarized light microscope, and confocal laser scanning fluorescence microscope. One of the samples collected at 12 weeks after the operation was decalcified. From this sample, the paraffin sections were prepared, stained with hematoxylin and eosin in the usual manner, and observed under a light microscope.

4. Estimation of bone areas in pores of the periosteum-attached HA block

The percentage of the total area of newly formed bones to the total area of pores that were observed as a circle, the percentage of the total area of bones formed in a pore to the pore area and the distance from the surface to which periosteum was attached to the center of the pore in the preparation were calculated for the purpose of objectively evaluating bone formation in pores with time. Following fur-

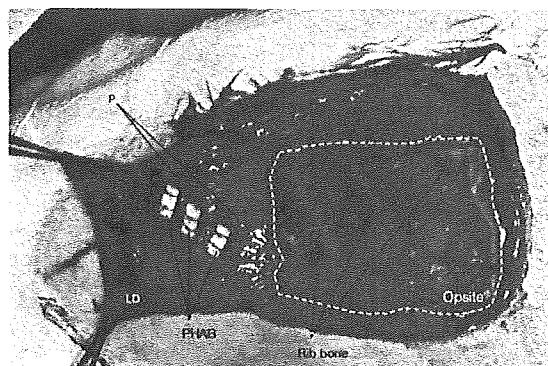


Fig. 1 : PHA blocks (porosity : 50%, dimensions : $8 \times 4 \times 2$ mm) were ligatned to the cambium layer of periosteum and muscle followed by the raising of the latissimus dorsi musculo-periosteal flap. Strips of periosteum, each 3-5 mm in width and 25-30 mm in length, were obtained from 8th to the 11th ribs.

ther observations by light microscopy, the microscopic images were inputted via a digital camera (PDMC Ie, Polaroid Corporation, USA) as digital images (800×600 pixels) (TIFF format) in to a personal computer (PowerBook G4, Apple Computer Inc., USA). There were approximately 130 pores per preparation for a total of 4000 pores in 30 preparations. The area of each pore and the area of newly formed bone in the pore were determined using image analysis software (Image J, freeware downloaded from <http://rsb.info.nih.gov/ij/>), and the percentage of the total area of newly formed bones in the pores to the total area of the pores was obtained in each preparation. The percentage of the area of bones formed in one pore to the pore area and the distance from the surface to which the periosteum was attached were analyzed using single regression analysis for the purpose of evaluating the progression of new bone formation in PHAB.

5. Evaluation of tissues formed in pores

The area of each tissue observed in pores

was determined in the preparations of the periosteum- and muscle-attached blocks, and the percentage of the area of each tissue to the total area of newly formed tissues was compared between these preparations.

6. Evaluation of three-dimensional (3D) distribution of tissues in pores

The pore that is observed as a circle in a preparation is a given cross-section of the pore that can be hypothesized as a sphere. The following parameters were estimated to show the 3D distribution of each tissue in a pore. The percentage of each area representing bone, adipose, and fibrous connective tissues in each pore and the area of the pore were estimated using image analysis software (Image J). Deviation ratios (DR) were obtained by dividing the radius (r) of a pore circle (d : area of each circle) in each preparation by the maximum radius (R : radius of the largest circle observed), estimated from the radius of the largest circle, to establish how far it was from the circle observed to the center of the sphere. The equations using “ d ” and “ D ” values which can be obtained by the morphometric analysis program were as follows :

$$r^2 + l^2 = R^2$$

$$D = \pi R^2$$

$$l = \sqrt{(R^2 - r^2)}$$

$$\text{Deviation Ratio (DR)} = l/R = \sqrt{(R^2 - r^2)}/R =$$

$$\sqrt{(D-d)/D} = \sqrt{(1-d)/D}$$

Then, the percentages of the areas of bone and adipose tissue in each pore were calculated. The determination and evaluation were conducted under the hypothesis that a pore was a sphere and evenly distributed in a block and each pore observed in a preparation was a perfect circle.

Results

1. Histological evaluation

In the periosteum-attached block, approximately half of the pores in PHAB were filled with loose and edematous fibrous tissues at 4 weeks after the operation (Fig. 2A), but the rest were vacant. At 8 weeks after the operation, most of the pores in the preparation were filled with loose fibrous tissues with vascularization, and formation of calcified bones was observed in only part of the pores (Fig. 2B). At 12 weeks after the operation, all of the pores were filled with fibrous connective tissue, and bone and adipose tissue was also observed in some pores (Fig. 2C). In these pores, fibrous connective and adipose tissues were observed in the center of the pores, and bone was observed along the wall of the pores. It was confirmed that these bones had a laminated architecture, which showed birefringence in polarized light microscopy, and were mature calcified bone tissues that emitted green fluorescence at an excitation wavelength of 520 nm (Fig. 2D). Observation with confocal laser scanning fluorescence microscopy revealed calcified bones that emitted green fluorescence at an excitation wavelength of 520 nm at the site corresponding to the area of bone observed under a light microscope (Fig. 3). Blood vessels running through the connecting passage between pores were also observed in some preparations. In the observation of decalcified preparations, the accumulation of cells with a small basophilic nucleus, corresponding to an islet of erythroblasts, was often found in some adipose tissues (Fig. 4).

In the muscle-attached HA block, formation of fibrous connective tissue was observed throughout the experimental period and no formation of new bones and adipose tissue

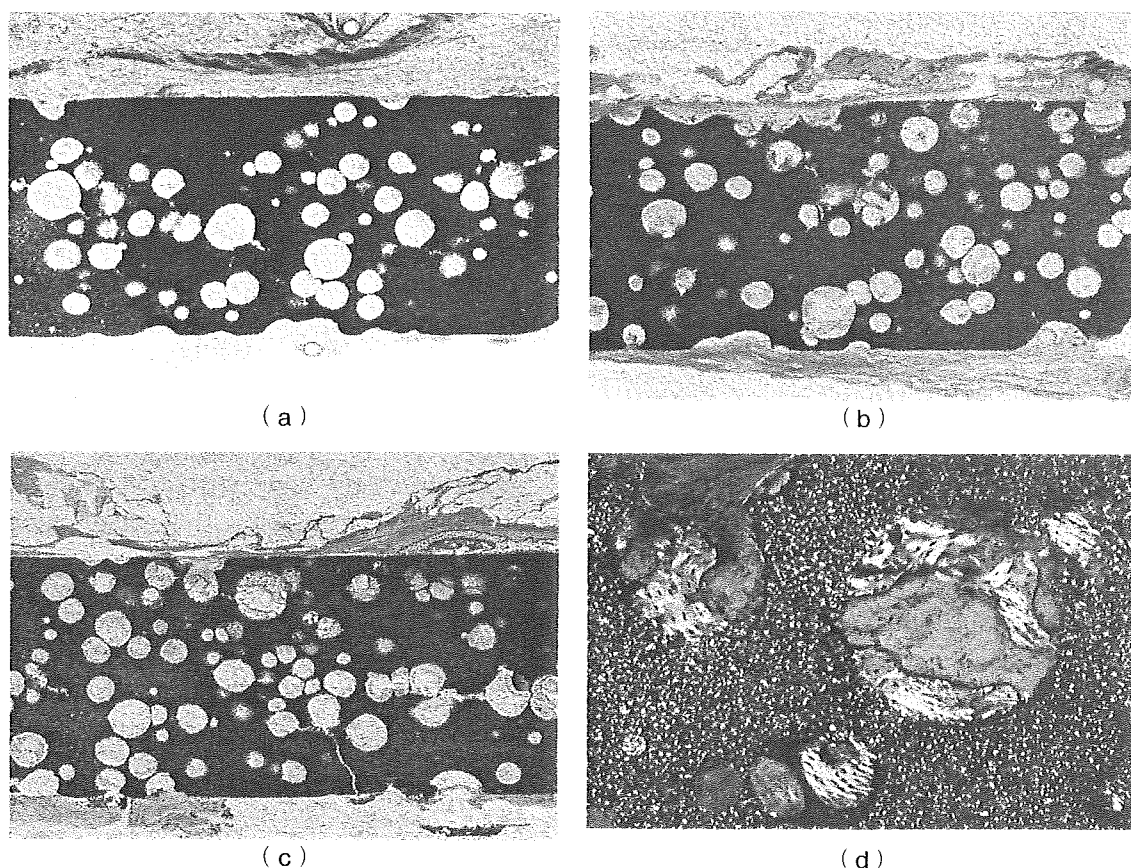


Fig. 2 : Low power view of the pores of non-decalcified ground sections with attached periosteum. (a) Pores were almost vacant 4weeks after implantation. (b) Pores were entirely filled with fibrous tissue and some of them included bone islets at 8 weeks. (c) Bone formation gradually progressed in the pores near the attached side of the periosteum at 12 weeks. (a~c) : Villanueva bone stain, $\times 40$ (d) Especially, double-refracted, laminated, and mineralized bone was found in the pores by polarizing microscope at 12 weeks. (Villanueva bone stain, $\times 100$)

was observed in the pores (Fig. 5).

2. Changes in areas of bone in the pores of the periosteum-attached blocks

In the periosteum-attached PHAB, no bone formation was observed in any of the pores in the preparations at 4 weeks after the operation. However, the mean percentage of bone area to the pore area in the preparations at 8 weeks after the operation reached 2.00% and the maximum value was 7.66%. The mean percentage reached 3.15% and the maximum

value was 15.1% in the preparations at 12 weeks after the operation (Fig. 6). In the muscle-attached PHAB, no bones were found in any pores in the preparations throughout the experimental period.

In the blocks obtained at 12 weeks after the operation, the preparations were listed in descending order of percentage of bone area, and four preparations with higher percentages of bone area were selected. In these preparations, the percentage of bone area in a pore to the pore area and the distance from

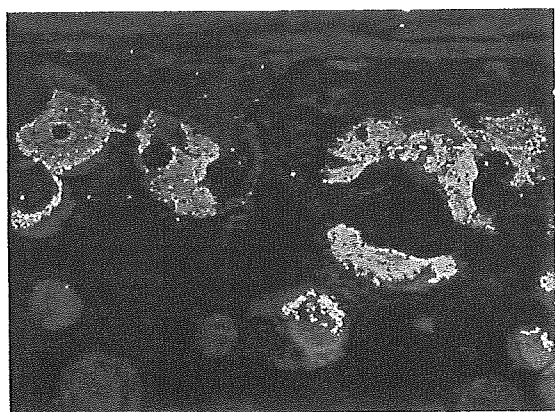


Fig. 3 : Low power view and confocal laser fluorescence micrograph of the laminated bone at 12 weeks with attached periosteum. Bone formation was observed along the wall of the pores, and we confirmed that these bones had a laminated structure, which showed birefringence in polarized light microscopy and were mature calcified bone tissues that emitted green fluorescence at an excitation wavelength of 520 nm. (Villanueva bone stain, $\times 40$)

the surface to which periosteum was attached were tested by single regression analysis. A negative linear correlation between these parameters was obtained from all of these preparations (Fig. 7~10). Pearson's product moment correlation coefficient was obtained from the data of all the pores in the preparations of the blocks collected at 12 weeks after the operation and tested by z transformation. As a result, there was a negative correlation of -0.279 ($p < 0.001$, $n = 1038$) between the percentage of new bone formation in each pore and the distance from the attached periosteum (Fig. 11).

3. Percentages of tissues in a pore

The percentage areas of each component tissue observed in a pore were compared between the periosteum- and muscle-attached blocks. In the periosteum-attached block, the percentage of bone and adipose tissues was as

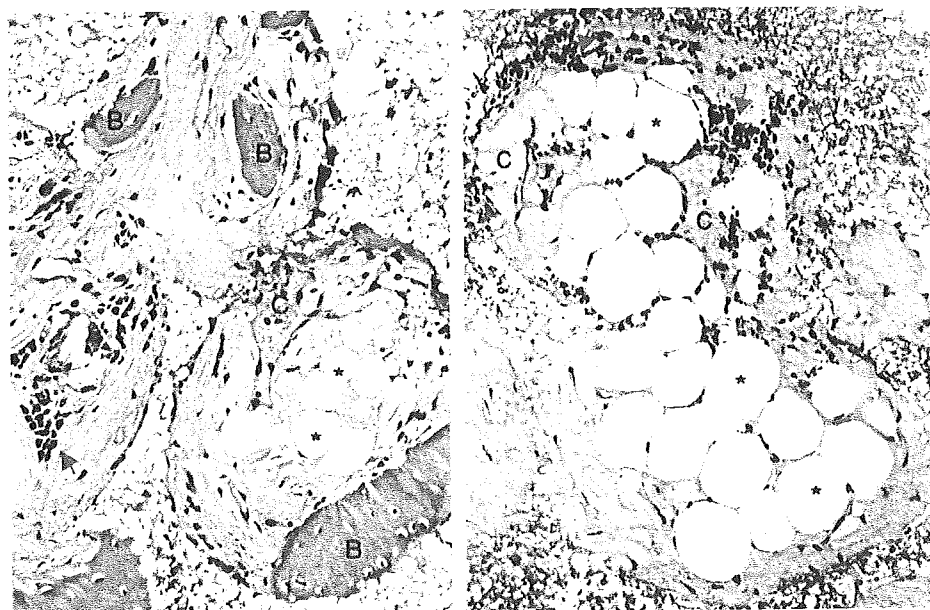


Fig. 4 : High power view of the pores, decalcified section at 12 weeks. Blood vessels running through the interporous canal between pores are present. The accumulation of cells with a small basophilic nucleus, i.e., an islet of erythroblasts, was often found in some adipose tissues. (HE stain, $\times 100$. Arrow head ; Islets of erythroblasts, * ; Adipocytes, B ; Bone, C Capillary)

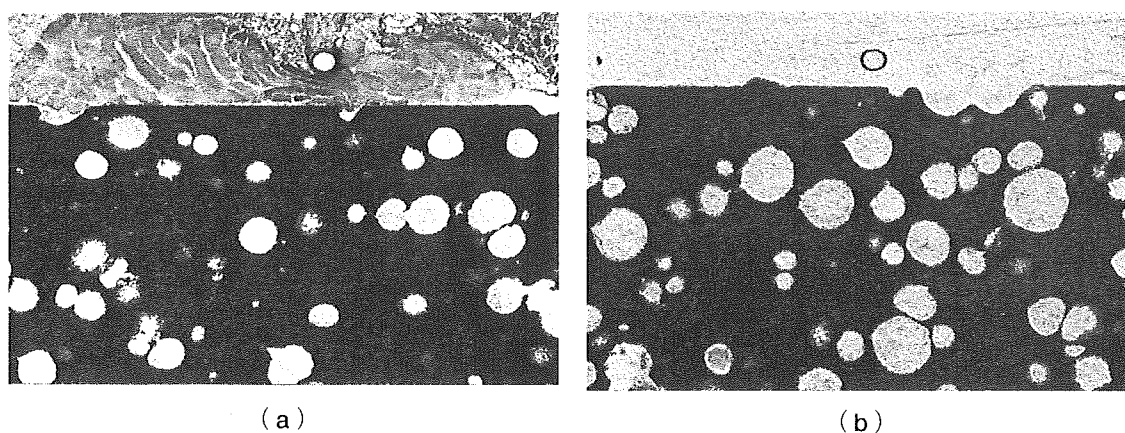


Fig. 5 : Low power view of the pores of non-decalcified ground sections with attached muscle. (a) The pores were entirely vacant at 4 weeks. (b) The pores were filled only with fibrous tissue at 12 weeks after implantation. (Villanueva bone stain, x40)

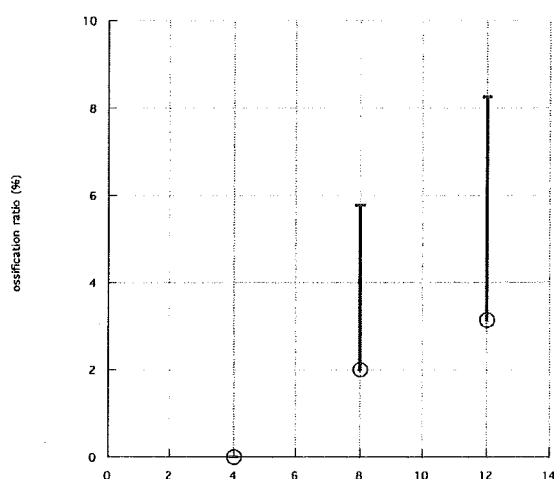


Fig. 6 : Sequential changes of the percentage bone area of the periosteum-attached blocks. No bone formation was observed in any of the pores in the preparations at 4 weeks after the operation, but the mean percentage of bone area to the pore area in the preparations at 8 weeks after the operation reached 2.00% and the maximum value was 7.66%. The mean percentage reached 3.15% and the maximum value was 15.1% at 12 weeks after the operation.

high as 5 %, and that of fibrous tissues including blood vessels was approximately 83%. In the muscle-attached block, only blood vessels and fibrous tissues were observed, and neither bone nor adipose tissues was found (Fig.

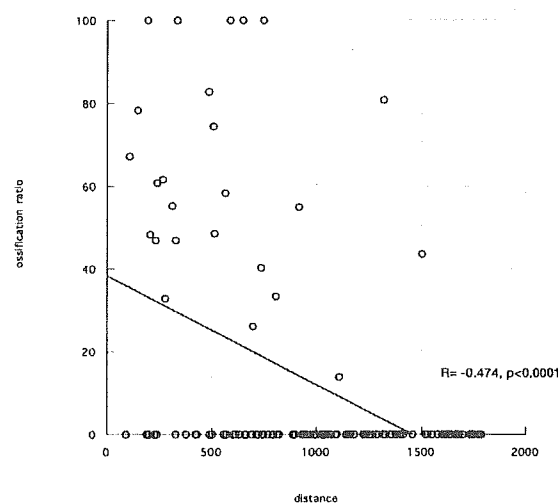


Fig. 7 : All graphical representation with analytical results of Pearson's product moment correlation coefficient of the pores with attached periosteum.

12).

4. 3D distribution of each tissue in a pore

Bone tissues were observed along the circumference of a pore as approximately 10% of the radius in width, and adipose tissues were often demonstrated on the inner side of the bone tissue as approximately 10% of the radius in width. Only fibrous tissues including

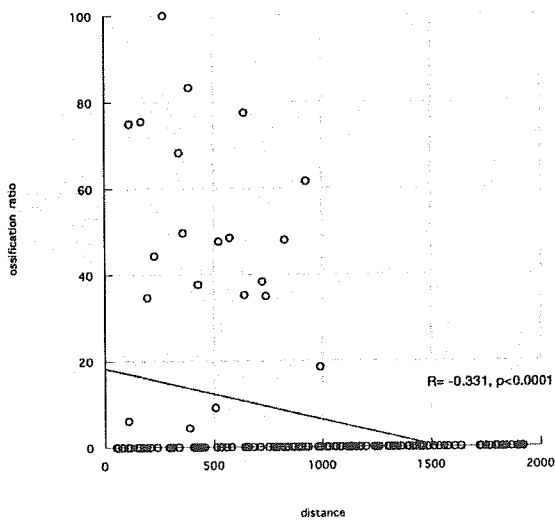


Fig. 8 : All graphical representation with analytical results of Pearson's product moment correlation coefficient of the pores with attached periosteum.

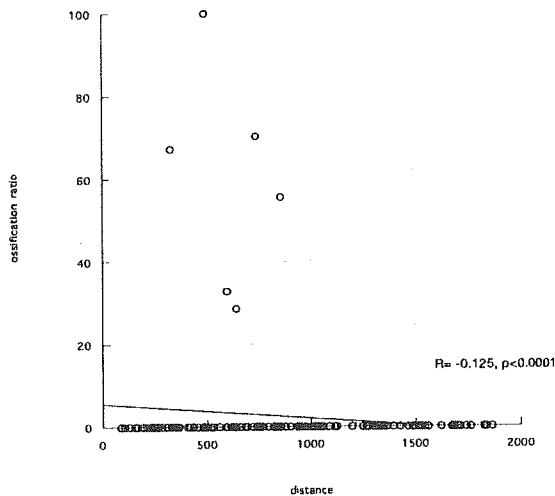


Fig. 10 : All graphical representation with analytical results of Pearson's product moment correlation coefficient of the pores with attached periosteum.

blood vessels were observed from the center to approximately 80% of the radius (Fig. 13).

Discussion

Although autologous bone graft, especially vascularized bone graft, has been regarded as one of the most reliable procedures for repair-

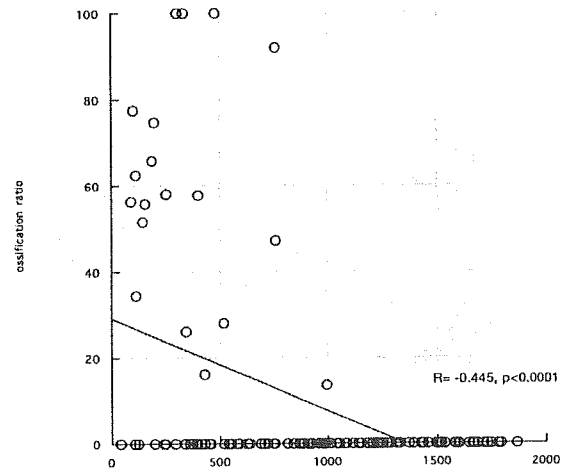


Fig. 9 : All graphical representation with analytical results of Pearson's product moment correlation coefficient of the pores with attached periosteum.

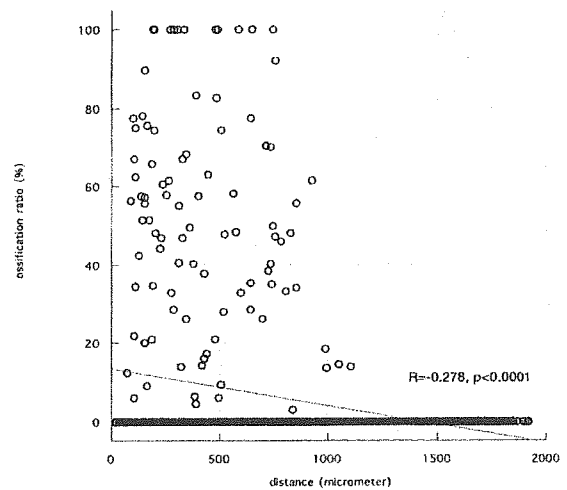


Fig. 11 : Integrated graphical representation with analytical results of Pearson's product moment correlation coefficient tested by z transformation. This result shows a negative correlation of -0.279 between the percentage of new bone formation in each pore and the distance from the attached periosteum. ($p < 0.001$, $n = 1038$)

ing bone defects after major surgical intervention and/or trauma, it is still hard to gain sufficient volume, strength, and shape of autologous bone grafting in cases of bone defects that are large and complicated in shape. Various materials have been recently proposed for

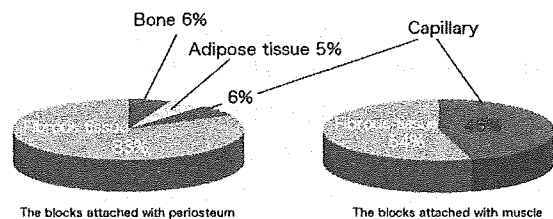


Fig. 12 : The percentages of areas of tissues observed in a pore were compared between the periosteum- and muscle-attached blocks. The percentage of fibrous connective tissues including blood vessels was as high as 83% and that of bone and adipose tissues was approximately 5% in the periosteum-attached block. On the other hand, only blood vessels and fibrous connective tissues were observed, and no bone and adipose tissues were found in the muscle-attached block.

replacing autologous bone graft, such as metallic materials, inorganic substances like HA, macromolecular polymers or biopolymers⁸⁾. Among them, HA has been regarded as one of the promising candidates of artificial bone for clinical use because it has suitable biological affinity and has been known to promote the differentiation of stem cells into osteoblasts⁹⁾.

We investigated the possibility of using vascularized periosteum-attached PHA as a novel material for replacing bone defects. We previously reported that osteogenesis had been confirmed in the pores of PHAB, which had been attached to the anterior portion of detached periosteum, having no connection to intercostal vessels¹⁰⁾. A hypothesis emerged from the study that PHAB could be regarded as one of the most favorable materials for bone reconstruction, because PHAB is easily processed to fit the shape of the each defect, and a scaffold comprising PHAB filling the defect would retain its shape while bone formation in the pores is completed. There have been several experimental studies emphasizing the success of mature bone formation in

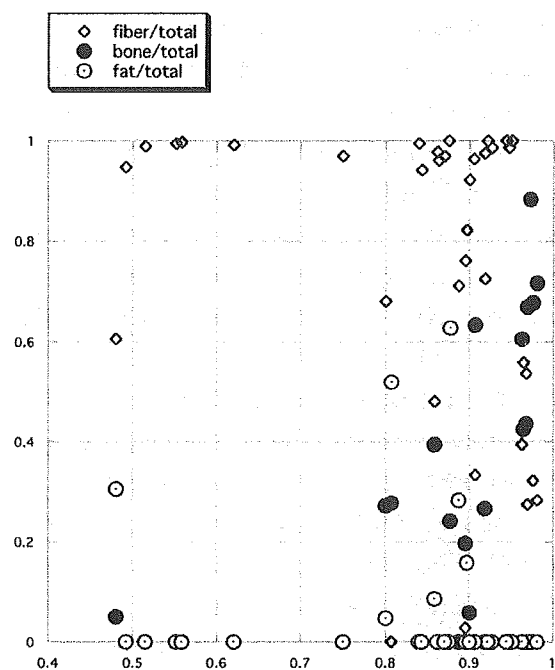


Fig. 13 : Evaluation of the 3-D distribution of each tissue in a pore at 12 weeks after implantation. The horizon indicates the deviation ratio (DR), and the vertical shows areas of induced tissue in the pores. Bone tissues were observed along the circumference of a pore as approximately 10% of the radius in width, and adipose tissues were often observed on the inner side of the bone tissue as approximately 10% of the radius in width. Only fibrous connective tissues including blood vessels were observed from the center to approximately 80% of the radius.

granules or blocks of HA which had been embedded in soft tissue, followed by the entire covering of vascularized periosteum^{11,12)}. However, few described sequential examinations of bone induction in the pores of PHAB in detail. Therefore, we aimed to discuss here-with the sequential events of osteogenesis in pores with attached periosteum, on the basis of results from detailed microscopic observations and morphometric analysis.

In this study, newly formed bone was confirmed to have a laminated architecture and depolarization was initially found at the margin of the pores near the face of the block

attached to by periosteum at week 8 after the surgical intervention, and bone formation in pores extended to the distal portion from the attached face of PHAB of rectangular shape. At week 12, adipose tissue containing islets of erythroblasts were usually observed inside the bone, recognized as bone sloughing lining the pore. The percentage of fibrous tissues including blood vessels was as high as 83% and that of bone and adipose tissues was 5%. By contrast, neither bone nor adipose tissue was found in the pores of PHAB embedded in the muscle during the entire experimental period. The result provides evidence that bone and adipose tissue containing islets of erythroblasts always appeared together only in pores of periosteum-attached PHAB.

To study in more detail the relationship between bone formation and the functioning of periosteum attachment, the ratio of bone area to the total area of all pores was examined. There was a significant increase in the mean ratio of bone area to pore area in all preparations from 8 weeks after the operation. Then, morphometric analysis revealed a negative correlation of -0.279 ($p < 0.001$, $n = 1038$) between the percentage of bone in each pore and the distance from the face of PHAB-attached periosteum. It is known that the periosteum of animals contains subsets of progenitor cells that possess the potential to differentiate directly into osteoblasts when inoculated *in vivo*¹³⁾. Accordingly, periosteum may act as a source of stem cell supply and cause bone formation in the pores of PHA extending in a direction away from the periosteum-attached face of PHAB.

Consistent with these results, adipose tissue can be recognized as a part of newly developed bone marrow, because most of the adipose tissue formed in sloughed bone contained islets of erythroblasts regarded as an impor-

tant component of hematopoiesis. This notion is also supported by a study that stated the potential of mesenchymal stem cells to differentiate into bone, fat, and muscle¹⁴⁾. Therefore, the two components newly developed in the pores, bone and adipose tissue, must be induced by differentiation of mesenchymal stem cells provided via periosteum which must function to accumulate and deliver circulating stem cell to pores in adjacent PHAB because of the failure of bone formation in muscle-attached PHAB¹⁵⁾. Although evidence of mesenchymal stem cells was not confirmed in the study, the result of formation of bone sloughing containing adipose tissue with a hematopoietic system in pores of PHAB, assumes that the periosteum was an essential component, acting as a source of stem cells to induce mature bone in the pores.

On the other hand, it has been generally discussed that the structural configuration of HA including the size and shape of the pores within the fabricated scaffold, has been shown to be critical in allowing osteoinduction and growth of bone itself into the scaffolds whilst also allowing the transfer of nutrients through the scaffold^{16,17)}. The present study also elucidated that the thickness of bone, adipose tissue, and fibrous tissue in the spheres of the pores might develop from the outer layer to the center of the radius in the ratio of 10-10-80 of radius by the concise stereological analysis of each component in pores. Generally, PHAB designed with 50-60% porosity and a pore size ranging from $100\ \mu\text{m}$ to $400\ \mu\text{m}$ in diameter has been considered optimal for bone formation^{18~20)}. Factors affecting the porosity of the scaffolds must be taken in to consideration and be balanced with the mechanical strength of the scaffold as a requirement of tissue engineered scaffolds is that they must have sufficient mechanical strength for the application

they are designed for²¹⁾. The results of the present study suggest that smaller pore diameters in PHAB may increase bone volume and provide favorable osteoinduction and sufficient strength.

As a conclusion, bone and adipose tissue containing islets of erythroblasts in pores may be induced by differentiation of mesenchymal stem cells provided via the periosteum which may play an important role to accumulate and deliver stem cells to pores in adjacent PHAB. Even if the clinical application of PHAB alone is still limited because of the difficulty to establish sufficient strength to replace the defect and prevent infection, we wish to emphasize that the complex of PHAB-attached vascularized periosteum presented in this study may become a favorable and secure material for bone reconstruction *in vivo*.

Acknowledgements

We are indebted to Ms. Yoko Maeda for her devoted technical assistance. We would like to thank Mr. Takehiko Nakajima and his co-worker (PENTAX Co. Ltd.) and Mr. Inoguchi (Hard tissue Co. Ltd.) for their helpful discussion and material assistance. A part of this work was supported by a Grant-in-Aid (No. 16591803) for Scientific Research from the Ministry of Education, Science, Sports and Culture of Japan and by a Project Research Grant from Toho University School of medicine (No.19225).

References

- 1) Maruyama Y, Onishi K, Iwahira Y, et al. : Free compound rib-latissimus dorsi osteomusculocutaneous flap in reconstruction of the leg, *J Reconstr Microsurg*, **3** : 13~18, 1986.

- 2) Maruyama Y, Urita Y, Ohnishi K : Rib-Latissimus dorsi osteomyocutaneous flap in reconstruction of a mandibular defect, *Br J Plast Surg*, **38** : 234~237, 1985.
- 3) Finley JM, Acland RD, Wood MB : Revascularized periosteal grafts -A new method to produce functional new bone without bone grafting, *Plast Reconstr Surg*, **61** : 1~6, 1979.
- 4) Puckett CL, Hurvitz JS, Metzler MH, et al. : Bone formation by revascularized periosteal and bone graft, *Plast Reconstr Surg*, **64** : 361~365, 1979.
- 5) van den Wildenberg FA, Goris RJ, Tutein Nolthenius-Puylaert MB : Free revascularised periosteum transplantation : an experimental study, *Br J Plast Surg*, **37** : 226~235, 1984.
- 6) Canalis RF, Burstein FD : Osteogenesis in vascularized periosteum. Interactions with underlying bone, *Arch Otolaryngol*, **111** : 511~516, 1985.
- 7) Ono I, Suda K, Takeshita T, et al. : Analysis of strength and bone conduction of hydroxyapatite ceramics, *J.Jpn. P.R.S.*, **13** : 561~571, 1993.
- 8) Boyan BD, Hummert TW, Dean DD, et al. : Role of material surfaces in regulating bone and cartilage cell response, *Biomaterials*, **17** : 137~146, 1996.
- 9) Ohgushi H, Dohi Y, Yoshikawa T, et al. : Osteogenic differentiation of cultured marrow stromal stem cells on the surface of bioactive glass ceramics, *J Biomed Mater Res*, **32** : 341~348, 1996.
- 10) Hirata A, Maruyama Y, Hayashi A, et al. : Study on osteogenesis in artificial bone comprised of the porous hydroxyapatite block with attached rib-latissimus dorsi periosto-muscle flap in rabbit, *J Med Soc Toho*, **52** : 212~219, 2005.
- 11) Takato T, Harii K, Nakatsuka T, et al. :